

Now one may calculate the Boltzmann averages of these internal fields, i. e.,

$$\langle \vec{H}_{\text{int}} \rangle_T = \sum_n \langle n | \vec{H}_{\text{int}} | n \rangle e^{-\beta E_n} / \sum_n e^{-\beta E_n}$$

so that the nucleus sees the effective field as the vector sum

$$\vec{H}_{\text{eff}} = \langle \vec{H}_{\text{int}} \rangle_T + \vec{H}_{\text{applied}}. \quad (\text{A5})$$

*Work supported in part by National Science Foundation and the Office of Naval Research.

¹P. Zory, Phys. Rev. **140**, A1401 (1965); J. T. Schriempf and S. A. Friedberg, *ibid.* **136**, A518 (1964); C. E. Johnson and M. S. Ridout, J. Appl. Phys. **38**, 1272 (1967); K. Ono, M. Shinohara, A. Ito, T. Fujita, and A. Ishigaki, *ibid.* **39**, 1126 (1968).

²R. Ingalls, K. Ono, and L. Chandler, Phys. Rev. **172**, 295 (1968).

³W. T. Oosterhuis and G. Lang, Phys. Rev. **178**, 439 (1969).

⁴J. M. Baker, B. Bleaney, and K. D. Bowers, Proc. Phys. Soc. (London) **B69**, 1205 (1956); B. Bleaney and

M. C. M. O'Brien, *ibid.* **B69**, 1216 (1956).

⁵C. A. Helcke, D. J. E. Ingram, and E. F. Slade, Proc. Roy. Soc. (London) **B169**, 275 (1968).

⁶The basis states are chosen to be $|a, m\rangle$, $|b, m\rangle$, and $|c, m\rangle$ so that the matrix elements of \mathcal{H}_0 are real.

⁷O. M. Jordahl, Phys. Rev. **45**, 87 (1934).

⁸One can easily obtain the transformation $\frac{1}{2}(V_{xx} - V_{yy}) \pm iV_{xy} = \frac{1}{2}(V_{\bar{x}\bar{x}} - V_{\bar{y}\bar{y}}) e^{\pm 4i\gamma}$ by calculating $V_{ij} = \delta^2 V / \delta x_i \delta x_j$, using the chain rule and the transformation between (xyz) and $(\bar{x}\bar{y}\bar{z})$, which are separated by an angle of 2γ about a common z axis.

⁹G. Lang, Quart. Rev. Biophys. **3**, 1 (1970); C. E. Johnson, Proc. Phys. Soc. (London) **92**, 748, (1967).

Effect of Iron Impurities on the Thermal Conductivity of Magnesium Oxide Single Crystals below Room Temperature

I. P. Morton

Physics Department, University of Southampton, Southampton, England

and

M. F. Lewis

General Electric Company Ltd., Central Research Laboratories, Hirst Research Centre, Wembley, Middlesex, England
(Received 20 October 1969)

The thermal conductivity between 5 and 300 °K of magnesium oxide single crystals containing different amounts of iron impurity has been measured. The iron produces a marked reduction in the thermal conductivity with a minimum at around 80 °K in the highly doped (~1%) samples and we attribute this effect to resonant scattering of phonons of energy $\sim 105 \text{ cm}^{-1}$ interacting with two groups of magnetic levels of the Fe^{2+} ions. We have estimated the strength of the interaction from earlier spin-lattice relaxation-time measurements. Using an expression due to Callaway for the frequency dependence of the basic phonon heat current, we have then computed the effect of this interaction on the thermal conductivity. We find that we can account substantially for the observed data by using for the resonant interaction a Lorentzian line shape with a full characteristic width equal to that observed in infrared experiments (9 cm^{-1}), but cut off at nine times the width.

I. INTRODUCTION

The theory of the thermal conductivity of dielectric solids attributes the heat transport to thermal phonon wave packets.¹ Each wave packet is characterized by a frequency ω , a mean wave vector \vec{q} (and polarization p , usually uniquely determined by ω and \vec{q}), and a relaxation time $\tau(\omega, \vec{q})$ arising from non-wave-vector conserving processes.² In a certain approximation, the thermal conductivity is given by the following sum of contributions from the wave packets comprising the thermal phonon field¹:

$$K = \frac{1}{3} \sum_{\omega, \vec{q}} C(\omega, \vec{q}) v^2(\omega, \vec{q}) \tau(\omega, \vec{q}), \quad (1)$$

where $C(\omega, \vec{q})$ is the specific heat per unit volume and $v(\omega, \vec{q})$ is the group velocity of the thermal phonons.

The principal problem in the theory of thermal conductivity is to compute the quantity $\tau(\omega, \vec{q})$, since it is virtually impossible to invert Eq. (1) directly so as to deduce $\tau(\omega, \vec{q})$ from measurements of K . The best that one can normally hope to achieve is a demonstration that the measurements of K are consistent with a particular calculated form of $\tau(\omega, \vec{q})$. For example, the extensive measurements and complicated analysis of Berman and Brock³ have produced a consistent explanation for the contribution of isotope scattering to the thermal resistance of LiF. Other scattering mechanisms in-

clude boundary, impurity, dislocation, and phonon-phonon umklapp processes.

In the present paper we present the results of some experimental measurements, partially reported earlier,⁴ and some calculations on MgO:Fe⁺⁺. We show that it is possible to give a consistent explanation for an observed thermal conductivity minimum at about 80°K in MgO:0.75% Fe in terms of a resonant thermal phonon scattering mechanism involving the ground and low-lying excited states of the Fe⁺⁺ ion. These states are separated by an energy corresponding to 150°K.⁵ Although such an explanation has previously been proposed to account for the observed reduction in the thermal conductivity in zero magnetic field of MgAl₂O₄⁶ and CdTe⁷ when doped with Fe⁺⁺, we believe that ours is the first quantitative analysis which employs the known energy levels of the excited states of the impurity ion (as deduced from infrared spectroscopy⁵ and spin-lattice relaxation-time measurements⁸), and also the known spin-phonon coupling⁸ deduced from measurements of the Orbach contribution to the spin-lattice relaxation.⁹ We find that the inclusion of the effect of normal processes is essential and we have done this by the methods of both Klemens¹ and Callaway.¹⁰ As a byproduct of the analysis we obtain some information on the line shape of the resonant spin-phonon interaction. In the Appendix we have also compared the linewidth of the spin-photon interaction measured by infrared spectroscopy with that expected from the various broadening mechanisms. At 20°K the calculated linewidth is ~7 cm⁻¹ compared with the measured width of ~9 cm⁻¹.

II. EXPERIMENTAL

The MgO:Fe⁺⁺ samples were grown by the arc fusion technique and were obtained from W. & C. Spicer Ltd., England. It was established from the Mössbauer spectrum that >90% of the iron in the highly doped specimen 9 was in the divalent state. The thermal conductivity apparatus is standard employing rod-shaped samples heated at one end by a constantan heater and attached to a heat sink at the other end. The temperature and temperature gradient are measured by Au:Fe versus Chromel thermocouples soldered to copper bands glued at two points along the length of the specimen.

The absolute values of the conductivity are only accurate to about 20% due to large uncertainties in the form factors, but, below 200°K the relative values of conductivity are accurate to better than 10%. Above 200°K a correction for radiation losses has been made which reduces the relative accuracy to 20%.

The results of the measurements are shown in Fig. 1. A pronounced minimum is clearly visible for the most highly doped sample which disappears

as the doping is reduced. Also, even allowing for the form factor uncertainty the conductivity at room temperature of the highly doped samples is reduced and we attribute this to increased point-defect scattering (see Sec. III).

III. THEORY

In all our calculations we have employed an isotropic Debye model of the MgO lattice using the following parameters: Mean molecular weight $M = 20.16$ g, density $\rho = 3.58$ g cm⁻³,¹¹ and a Debye temperature Θ_D varying from 945°K at $T = 0$ to 760°K at $T = 300$ °K.¹² This approximation reduces Eq. (1) to the form

$$K = \frac{2(kT)^3}{h^2\Theta_D} \left(\frac{6\pi^2 N_0 \rho}{M} \right)^{1/3} \int_0^{\Theta_D/T} \frac{x^4 e^x}{(e^x - 1)^2} \times \tau(x, T) dx, \quad (2)$$

where N_0 is Avagadro's number, $x = \hbar\omega/kT$, and $\tau(x, T)$ is a mean phonon relaxation time which depends upon the relaxation times of all possible scattering processes. The relaxation times which we shall consider for our doped single crystals are those due to (a) boundaries τ_b , (b) point defects $\tau_p(x, T)$, (c) umklapp processes $\tau_u(x, T)$, (d) normal processes $\tau_N(x, T)$,^{1,3,10} and (e) resonant scattering of phonons coupling with the magnetic energy levels of the Fe⁺⁺ impurities¹³ $\tau_r(x, T)$. We consider first the resonant contribution $\tau_r(x, T)$.

We estimate $\tau_r(x, T)$ from the expression given

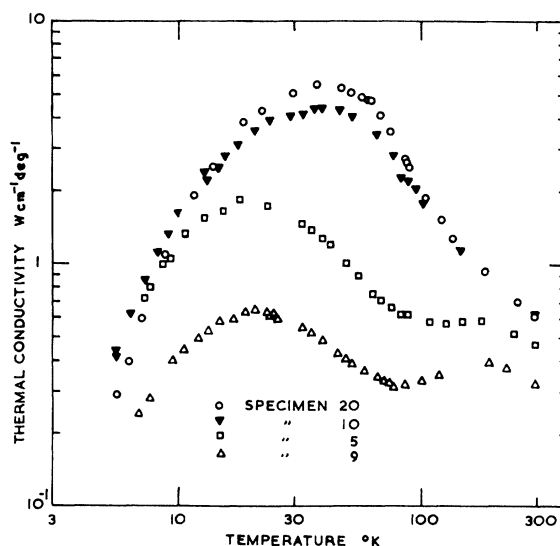


FIG. 1. Variation with temperature of the thermal conductivity of four specimens of MgO. Specimen 20 is nominally pure (99.9%) while specimens 10, 5, and 9 contain 300, 3000, and 7500 ppm Fe, respectively.

by Orbach^{13,14} for the phonon relaxation time due to direct processes between two states $|a\rangle$ and $|b\rangle$,

$$\tau^{-1}(\omega, T) = \frac{\pi}{\hbar} |\langle a | V_{01} | b \rangle|^2 \frac{\omega}{\rho v^2} g(\omega - \omega_0) \Delta N_s, \quad (3)$$

where $g(\omega - \omega_0)$ is the spin packet line-shape function, ΔN_s the spin population difference per unit volume between the states $|a\rangle$ and $|b\rangle$, $\hbar\omega_0$ the energy separation between the states, and V_{01} is a coupling operator.

In our calculations, we consider only transitions in zero applied magnetic field between the ground triplet Γ_{5g} and the next excited group of states Γ_{4g} and Γ_{3g} situated 105 cm^{-1} above the ground state.⁵ The ground triplet is split inhomogeneously by random crystal lattice strains¹⁵ into a singlet and doublet, and observations of the spin-lattice relaxation times within this triplet have been made.⁶ These measurements identify an Orbach relaxation process due to the presence of the Γ_{4g} and Γ_{3g} states with a relaxation time t_1 given by

$$t_1^{-1} = A \exp(-150/T), \quad A = 3 \times 10^{11} \text{ sec}^{-1}. \quad (4)$$

(There is an uncertainty of up to a factor of 3 in the measured value of A .) The matrix element in expression (3) can be related to A in the following way.

It can be shown¹⁶ that the spin-lattice relaxation time for spins relaxing between states $|a\rangle$ and $|c\rangle$ via the third state $|b\rangle$ is

$$t_1^{-1} = \frac{3\omega_0^3}{2\pi\rho v^5\hbar} \frac{2|\langle a | V_{01} | b \rangle|^2 |\langle c | V_{01} | b \rangle|^2}{|\langle a | V_{01} | b \rangle|^2 + |\langle c | V_{01} | b \rangle|^2} e^{-\hbar\omega_0/kT}, \quad (5)$$

where both kT and the energy separation between states $|a\rangle$ and $|c\rangle$ are very much less than $\hbar\omega_0$, the energy separation of $|b\rangle$. We make the further simplifying assumption that $|\langle a | V_{01} | b \rangle|^2 = |\langle c | V_{01} | b \rangle|^2$ and obtain

$$t_1^{-1} = (3\omega_0^3/2\pi\rho v^5\hbar) |\langle a | V_{01} | b \rangle|^2 e^{-\hbar\omega_0/kT}. \quad (6)$$

Here t_1^{-1} is proportional to the transition probability between states $|a\rangle$ and $|c\rangle$ via $|b\rangle$. If there are several states at $|b\rangle$ then the total transition probability, and hence relaxation time, will be the sum of the contributions from these states. In our system there are five excited levels at $\hbar\omega_0$ and so we can say

$$A = (3\omega_0^3/2\pi\rho v^5\hbar) \sum_e |\langle g | V_{01} | e \rangle|^2 \epsilon^{-1}, \quad (7)$$

where $|g\rangle$ is a ground state and $|e\rangle$ is one of the excited states. ϵ is a multiplying factor which arises from the fact that in our system the ground multiplet on which the relaxation-time measurements were made is a triplet and not a doublet. If the three levels are equally coupled to the excited levels then $\epsilon = 1$, but Ham¹⁷ has recently calculated all

the relevant matrix elements and finds ϵ should be $\sim 2-3$ depending on the exact distribution of the excited levels.

Returning to the estimate for the resonant contribution to the phonon relaxation time [Eq. (3)], we would expect that the over-all scattering probability to be due to the sum of the contributions from all possible transitions between ground and excited multiplets, i.e.,

$$\tau^{-1}(\omega, T) = \frac{\pi}{\hbar\rho v^2} \sum_{t=1}^{15} |\langle g | V_{01} | e \rangle|^2 \omega g_t(\omega - \omega_{0t}) \Delta N_{st}, \quad (8)$$

where the suffix t identifies the parameter with a given transition and the sum is over 15 possible transitions. The inhomogeneous broadening means that only a fraction $f'(\omega_{0t} - \bar{\omega}_{0t})d\omega_{0t}$ of the spins will have a set of possible transitions in the frequency interval $d\omega_{0t}$ centered around ω_{0t} and so ΔN_{st} in Eq. (8) becomes

$$\Delta N_{st} = N_s f'(\omega_{0t} - \bar{\omega}_{0t}) F(\omega_{0t}, T) d\omega_{0t}, \quad (9)$$

where

$$F(\omega_{0t}, T) = \frac{1 - \exp(-\hbar\omega_{0t}/kT)}{3 + 5 \exp(-\hbar\omega_{0t}/kT)} \quad (10)$$

is a population difference factor derived from Maxwell-Boltzman statistics, $\bar{\omega}_{0t}$ is the frequency of the maximum of the inhomogeneous line shape and N_s is the total number of spin centers present per unit volume.

Again the total relaxation time will be due to the sum of contributions from all the spins present in the specimen so that the phonon relaxation time becomes¹⁸

$$\tau^{-1}(\omega, T) = \frac{\pi}{\hbar\rho v^2} \int \sum_{t=1}^{15} |\langle g | V_{01} | e \rangle|^2 \omega N_s \times g_t(\omega - \omega_{0t}) f'(\omega_{0t} - \bar{\omega}_{0t}) F(\omega_{0t}, T) d\omega_{0t}. \quad (11)$$

The widths of the two line-shape functions g_t and f' can well be comparable (see Appendix), but they will both be very much less than $\bar{\omega}_{0t}$ so that we may take $F(\omega_{0t}, T)$, a slowly varying function, outside the integral and set it equal to $F(\bar{\omega}_{0t}, T)$. The remaining convolution integral just equals the full line-shape function $f(\omega - \bar{\omega}_{0t})$ centered about $\bar{\omega}_{0t}$ with a width approximately equal to the sum of the individual components.¹⁹ Then assuming

$$\sum_g \sum_e |\langle g | V_{01} | e \rangle|^2 = 3 \sum_e |\langle g | V_{01} | e \rangle|^2,$$

we obtain

$$\tau^{-1}(\omega, T) = 2\pi^2(v/\omega)^3 A \omega f(\omega - \bar{\omega}_0) N_s F(\bar{\omega}_0, T) \epsilon, \quad (12)$$

which in terms of $x = \hbar\omega/kT$ becomes

$$\tau_r^{-1}(x, T) = 2\pi^2 AN_s \epsilon (\hbar v / kT)^3 f(x - x_0) F(x_0) / x^2, \quad (13)$$

where $x_0 = \hbar \bar{\omega}_0 / kT$.

The forms assumed for the remaining contributions to the relaxation time are, for boundaries $\tau_b^{-1} = E_b$, for point defects $\tau_p^{-1}(x, T) = E_p x^4 T^4$, for umklapp processes $\tau_u^{-1}(x, T) = E_u x^a T^b \exp(-\theta_D / cT)$, and for normal processes $\tau_n^{-1}(x, T) = E_n x^d T^e$.¹⁰ The constants E_b , E_p , E_u , E_n , a , b , c , d , and e will be evaluated below.

We must now express the mean relaxation time $\tau(x, T)$ as a function of these individual times for insertion into Eq. (2). If we use the usual form

$$\begin{aligned} \tau^{-1}(x, T) &= \tau_b^{-1}(x, T) + \tau_p^{-1}(x, T) + \tau_u^{-1}(x, T) + \tau_r^{-1}(x, T) \\ &= \tau_i^{-1}(x, T) + \tau_r^{-1}(x, T) \end{aligned} \quad (14)$$

[the normal process term has been omitted since such processes do not directly attenuate the heat current¹ while $\tau^{-1}(x, T)$ has been split into a resonant term $\tau_r^{-1}(x, T)$ and a nonresonant intrinsic term $\tau_i^{-1}(x, T)$ for convenience], the results are unsatisfactory even for the case of no resonant scattering except at the lowest temperatures. This is well known and is due mainly to the fact that normal processes mix the phonon modes and reduce the validity of the derivation of Eq. (1).^{1,20,21} This failing is accentuated when resonant scattering is included when we find a predicted conductivity of entirely the wrong form to explain the results.

Klemens¹ overcomes this difficulty in an approximate way by assuming that $\tau_i^{-1}(x, T)$ is frequency independent for frequencies $\omega < kT/\hbar$ so that, with the inclusion of unmodified resonant scattering, the conductivity becomes

$$\begin{aligned} K(T) &= \frac{2(kT)^3 (6\pi^2 N_0 \rho / M)^{1/3}}{\hbar^2 \theta_D} \\ &\times \left(\int_0^1 \frac{x^4 e^x}{(e^x - 1)^2} [\tau_i^{-1}(1, T) + \tau_r^{-1}(x, T)]^{-1} dx \right. \\ &\quad \left. + \int_1^{\theta_D / T} \frac{x^4 e^x}{(e^x - 1)^2} [\tau_i^{-1}(x, T) + \tau_r^{-1}(x, T)]^{-1} dx \right). \end{aligned} \quad (15)$$

A later approach due to Callaway¹⁰ takes quantitative account of the normal processes. If we define a combined relaxation time

$$\tau_c^{-1}(x, T) = \tau_i^{-1}(x, T) + \tau_r^{-1}(x, T) + \tau_n^{-1}(x, T) \quad (16)$$

then the Callaway form of Eq. (2) becomes

$$\begin{aligned} K(T) &= \frac{2(kT)^3 (6\pi^2 N_0 \rho / M)^{1/3}}{\hbar^2 \theta_D} \int_0^{\theta_D / T} \frac{x^4 e^x}{(e^x - 1)^2} \\ &\times \tau_c(x, T) [1 + \beta \tau_n^{-1}(x, T)] dx, \end{aligned} \quad (17)$$

where

$$\begin{aligned} \beta &= \frac{\int_0^{\theta_D / T} \frac{\tau_c(x, T) x^4 e^x dx}{\tau_n(x, T) (e^x - 1)^2}}{\int_0^{\theta_D / T} \tau_n^{-1}(x, T) \left(1 - \frac{\tau_c(x, T)}{\tau_n(x, T)} \right) \frac{x^4 e^x dx}{(e^x - 1)^2}}. \end{aligned} \quad (18)$$

Expressions (15) and (17) are complex, but they are readily evaluated by computer and we have considered them both in an attempt to explain our results.

It now only remains to evaluate the constants in $\tau_i(x, T)$ and $\tau_n(x, T)$ and the expression for the full line shape $f(x - x_0)$. We have done this more or less empirically for each theory, but we confine our remarks for the time being to the theory of Callaway [Eq. (17)].

A. E_n , d , and e

An expression for the relaxation time due to normal processes at microwave frequencies can be found from ultrasound attenuation measurements. Such measurements²² at 3 GHz and on transverse polarizations (which should dominate the thermal phonon spectrum at low temperatures) indicate a normal process relaxation time τ_n given by

$$\tau_n^{-1} = F \omega (kT/\hbar)^4, \quad F = 10^{-57} \text{ sec}^4 \quad (19)$$

as the upper limit for τ_n . This gives the values $d = 1$, $e = 5$, and $E_n = 3.8 \times 10^{-2} \text{ sec}^{-1} \text{ } ^\circ \text{K}^{-5}$. Although these values are obtained at comparatively low frequencies and temperatures we assumed that d and e are the same at all frequencies and temperatures and that E_n will not change greatly. That this assumption is plausible is shown by the fact that a value of E_n of 8 times that above gives a good fit for the conductivity of our undoped specimen (specimen 20: see Fig. 2) and this is the value we have used throughout. A similar degree of agreement is produced by such an extrapolation in LiF and Al_2O_3 .²³

B. a , b , and c

Simple theories indicate²⁰ that $c \sim 2$ and usually c is chosen to give a good fit to observed conductivity data.⁷ The conductivity fit for the undoped specimen as well as the effect produced by resonant scattering in our calculations is found to be practically independent of c for $c \sim 2$ and so we have somewhat arbitrarily chosen a value of $c = 2$. Values of a and b are open to some debate,³ but we find that our results are insensitive to their exact values, largely¹⁰ because of the strong point-defect scattering, and we have used $a = 2$ and $b = 5$.

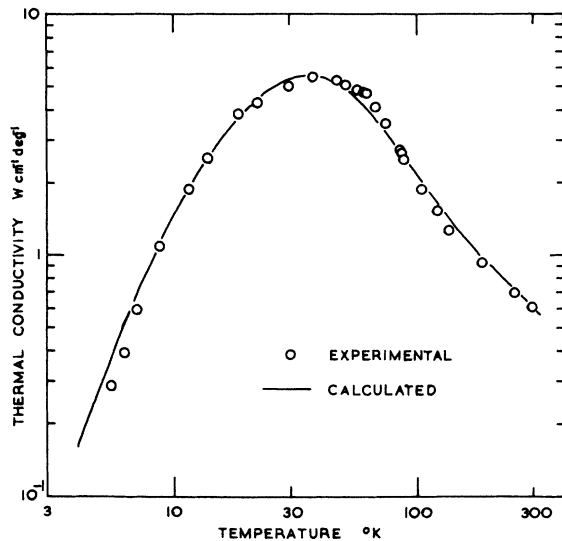


FIG. 2. Thermal conductivity variation with temperature calculated with the Callaway model for no resonant scattering compared with experimental data on specimen 20.

C. E_b , E_p , and E_u

These constants were evaluated entirely empirically in the following way.

The doped samples were manufactured from 99.9+% purity stock and so the intrinsic scattering $\tau_i(x, T)$ is assumed to be that of this material plus an extra point-defect contribution from the added impurities. There is some iron in the 99.9+% MgO (see Table I), but the closeness of the observed conductivities for specimens 20 and 10 indicate that the resonant contribution to the conductivity at these concentrations is small. The first step then is to set $\tau_r^{-1}(x, T) = 0$ in Eq. (16) and, for a given value of E_n , to alter E_b , E_p , and E_u to give a best fit to the measured conductivity of specimen 20. Computed and measured curves are compared in Fig. 2. Thus we now have E_b , E_u , and a value $E_p = E_{p1}$ for the undoped specimen. The above value of E_n was found by repeating this procedure for different values of E_n .

Computed conductivities using Eq. (17) and including resonant scattering show negligible reduction at room temperature due to the resonant term

TABLE I. Iron impurity in sample specimens.

Specimen No.	Fe impurity	Source
5	3000 ppm	GRC Ltd., England
9	7500 ppm	Spicer
10	300 ppm	Spicer
20	100 ppm (mean) (99.9% grade)	Spicer

and so we assume that the observed reduction at this temperature in the doped samples is due to enhanced point-defect scattering. (A recently measured MgO specimen containing $\sim 0.3\%$ Co shows a comparable reduction in room-temperature conductivity and so supports this assumption.) Using the earlier values of E_b and E_u the necessary value of E_p is found which gives the observed room-temperature conductivity for the doped sample (specimen 9). The increase is assumed to be proportional to N_s^{24} and so we have $E_p = E_{p1} + (E_{p2} - E_{p1})(N_s/7.5 \times 10^{20})$.

D. $f(x - x_0)$

Simple Gaussian and Lorentzian line shapes were tried at first. The Gaussian is too narrow and to achieve any kind of fit it is necessary to assume characteristic linewidths of several times the observed value. This indicates that a Lorentzian of the form

$$f(x - x_0) = 2(\Delta x) / \pi [(\Delta x)^2 + 4(x - x_0)^2]$$

where (Δx) is the full width at half-intensity, might be more suitable since it does not lose its strength so rapidly in the wings. Unfortunately this function extends too far into the wings so that the thermal conductivity is very strongly depressed at the lowest temperatures. As a result a compromise was chosen of a Lorentzian line cutoff in the wings at $(x - x_0) = w(\Delta x)$.²⁵ This relation defines the cutoff parameter w .

IV. COMPUTED RESULTS

Figure 3 shows a series of curves obtained by using Eq. (7) and a cutoff Lorentzian line shape. The series is for different levels of doping N_s , but

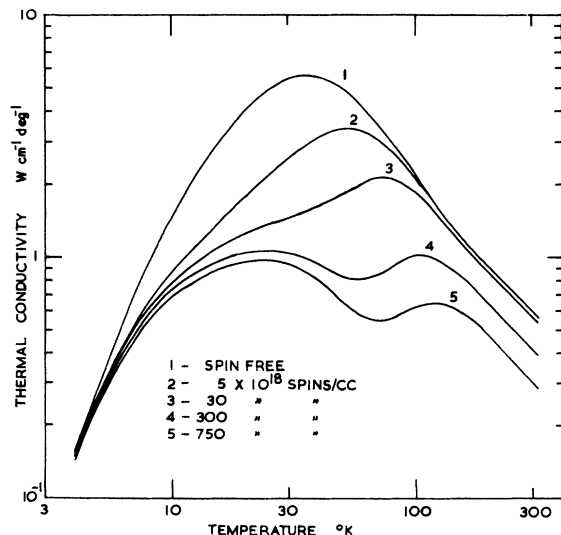


FIG. 3. Calculated thermal conductivity variation with temperature for different Fe²⁺ spin densities in MgO.

all other parameters are held constant with the following values: $E_h = 2.3 \times 10^7 \text{ sec}^{-1}$, $E_{p1} = 4.1 \text{ sec}^{-1} \text{ K}^{-4}$, $E_{p2} = 11.8 \text{ sec}^{-1} \text{ K}^{-4}$, $E_u = 0.05 \text{ sec}^{-2} \text{ K}^{-5}$, $E_n = 0.31 \text{ sec}^{-1} \text{ K}^{-5}$, $a = 1$, $b = 5$, $c = 2$, $A = 3 \times 10^{11} \text{ sec}^{-1}$, and $\epsilon = 3$. The resonant line used is centered at a frequency of $150k/\hbar$ with a full width at half-height of $13k/\hbar$ as observed in the infrared experiments,⁵ while the cutoff parameter used is $w = 9$. It can be seen that these curves show substantially the observed behavior although the observed minima occur at slightly too low a temperature and too large a depression of conductivity is produced at low temperatures for low doping levels. In order to obtain this fit we have allowed ϵ to vary up to 3 and no limitation on w . With E_n , E_b , E_{p1} , and E_{p2} and E_u fixed by the procedure detailed above, the effect of

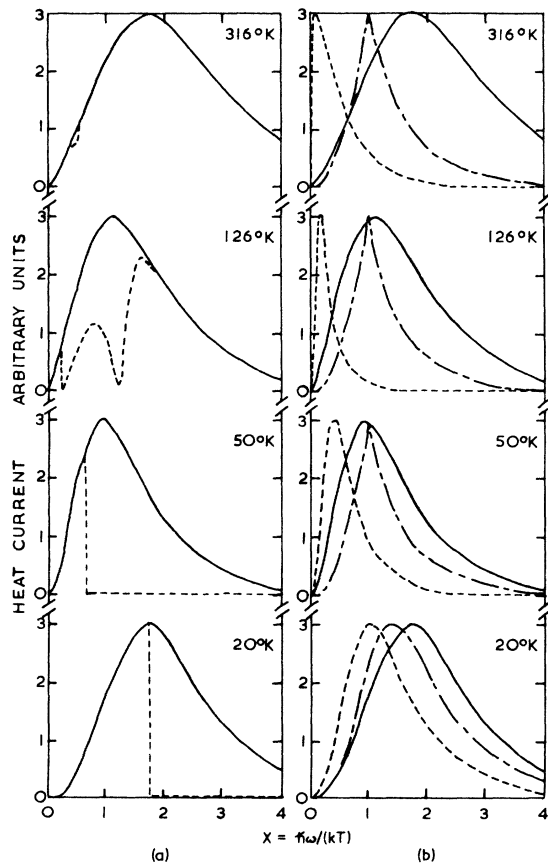


FIG. 4. Calculated heat current from phonons of frequency ω plotted as a function of $x = \hbar\omega/kT$ for four different temperatures. (a) Solid line: Callaway model with no resonant scattering; dashed line: Callaway model with 7.5×10^{20} spins per cm^3 . (b) Comparison of heat currents for no resonant scattering for three cases. Solid line: Callaway model; dot-dashed line: Klemens model; dashed line: no normal precesses. In each of these three cases the scattering parameters E_b , E_p , and E_u are such as to give a reasonable fit to the observed conductivity of specimen 20, and each is normalized separately.

these degrees of freedom can be seen from Fig. 4(a) where the contribution to the conductivity for phonons of frequency $\omega = xkT/\hbar$ is plotted against x for different temperatures. For each temperature two curves are shown, one for $N_s = 7.5 \times 10^{20}$ and the other for $N_s = 0$, but the doped value of E_p is used in both. Thus the difference between the two is entirely due to the resonant term and the ratio of the conductivities with and without resonant scattering will equal the ratio of the areas under the two curves. One can immediately make the following observations.

(i) At 316°K the spins affect the conductivity to a very small extent because of both the small value of (Δx) and the strong intrinsic phonon scattering. This is the justification for our procedure in choosing E_p .

(ii) At 126°K the intrinsic scattering and resonant scattering are of the same order and the resonant line has its full strength in approximately the same region as the maximum in the intrinsic curve. Consequently the reduction is sensitive to the strength of the resonant interaction A as well as the characteristic width of the line and the position of the intrinsic maximum.

(iii) At 50 and 20°K all phonon transport within the cutoff span $w(\Delta x)$ is effectively stopped, and this cutoff occurs near the intrinsic maximum and so the reduction depends on the span as well as the position of the maximum, but no longer on A .

We can summarize the effect of $w(\Delta x)$ and $A\epsilon$ as follows. At around 20°K the reduction is dictated almost entirely by $w(\Delta x)$ and allows this to be fixed, while by 126°K increases of both $A\epsilon$ and (Δx) decrease the conductivity.

Since the computed conductivity at 126°K is too high we have considered the effect of increasing $A\epsilon$. [Although there is some variation in observed inhomogeneous linewidths from specimen to specimen and so a variation in (Δx) could be considered, it is unlikely that the over-all width in our specimen differs substantially from that measured by Wong⁵ and so it is his value we have used in Fig. 3 (see Appendix).] With $\epsilon = 3$, however, A needs to be about 20 times the measured value to achieve the correct effect. This is well outside experimental error and a further failing of this approach is that, in increasing A , we exaggerate the resonant scattering at low temperatures in the weakly doped materials. The latter effect could, however, be due to the simplification of a sharp cutoff in the line shape.

Using the Klemens approach [Eq. (15)] gives substantially the same form for the predicted conductivity curves again with the minima at too low a temperature, but one can accommodate a lower value of A so that the scattering for weak doping is not quite so strong.

In Fig. 4(b) we compare the heat current frequency distribution curves on the Callaway and Klemens models as well as the case for no normal processes. The similarity of the Klemens to the Callaway distributions accounts for their close agreement in our computations.

So we see that the observed conductivity curves can be accounted for to a considerable degree although some details, in particular the fact that the predicted minima occur at too low a temperature, would require what seems, within the limitations of the theory, unjustifiable parameter fixing. The theory is however a simplification and has weaknesses which could account for the discrepancies and which we summarise as follows.

(a) The Callaway theory is an isotropic nondispersive one and does not take into account singularities in the phonon spectrum.

(b) One can envisage other forms of scattering which we have omitted from our calculations. These are Raman-type processes²⁶ attenuating nonresonant phonons, the possibility of Fe^{++} pairs²⁷ with their associated magnetic levels, and perhaps more importantly single ion magnetic levels higher than the Γ_{4g} and Γ_{3g} states giving further resonant scattering transitions.²⁸ These extra sources of magnetic scattering could give attenuation at frequencies higher than those we have used and so could account for the fact that our conductivity minimum occurs at too low a temperature. In addition they could provide an alternative to the effect of increased point-defect scattering used earlier to explain low room-temperature conductivities in heavily doped specimens. However, one point about high-frequency scattering sources which should be emphasised is that, because of the rapid decrease in the intrinsic nonresonant relaxation time with increasing frequency and temperature, any extra scattering must be correspondingly stronger in order to give an observable effect [Eq. (14)].

(c) A temperature-independent linewidth has been used on our program, although one might expect any lifetime broadened contribution to the width (see Appendix) to increase with increasing temperature because of phonon-stimulated emission. If such a temperature dependence is taken into account, however, the computed curves are altered very little and so, since the lifetime broadened contribution is somewhat uncertain, we have neglected the effect.

(d) Orbach's theory uses a Debye phonon spectrum and it also may become inappropriate for high magnetic ion concentrations.²⁹

V. CONCLUSIONS

By using a simple form for the frequency dependence of the heat current in dielectrics due to Callaway and Orbach's theory for the attenuation

of phonons in resonance with a paramagnetic spin system, we have been able to account, both qualitatively and quantitatively, for observed reductions in the thermal conductivity of MgO:Fe . Minor deviations do occur which we feel it would be interesting to resolve since this may well throw more light on the mechanisms of thermal conduction in the absence of resonant scatterers.

ACKNOWLEDGMENTS

One of us (M. F. L.) acknowledges useful discussions with Dr. F. S. Ham and Dr. G. A. Slack. Dr. G. A. Slack also informed us of his work on Fe^{++} in ZnS and CdTe prior to publication.

APPENDIX: WIDTH OF THE 105-cm^{-1} LINE

The width of the 105-cm^{-1} line was measured by Wong⁵ to be $\sim 9\text{ cm}^{-1}$ at 20°K and we have seen that such a width is also consistent with our thermal conductivity measurements. It is therefore of interest to see if such a width can be explained by other available data.

Three contributions to the linewidth will be considered separately.

(a) *Splitting of the $\Gamma_{5g} \rightarrow \Gamma_{4g}$ and $\Gamma_{5g} \rightarrow \Gamma_{3g}$ transitions.* Theoretically²⁸ this could be many cm^{-1} , but Wong's experiments apparently showed that it does not exceed $\sim 2\text{ cm}^{-1}$ since otherwise a resolved doublet would have been observed in the infrared spectrum.

(b) *Strain broadening.* This is known to be responsible for the measured widths of the electron-spin-resonance lines of several iron group ions in MgO .³⁰⁻³² Measurements of the strain broadened contribution to the ESR linewidths of the Mn^{++} and Fe^{+++} ions present in small amounts in our 0.75% Fe sample show it to be ~ 3 times as strained as purer samples we have measured.³² Using this fact together with Ham's result³³ that the excited states are five times as sensitive to strain as the ground states we deduce that the strain broadened width of each transition is $\sim 2\text{ cm}^{-1}$.

(c) *Lifetime broadening.* At low temperatures ($T < 150^\circ\text{K}$) this is determined by the spontaneous emission rate from the excited to ground levels and its magnitude can be estimated from the Orbach process contribution to the spin-lattice relaxation time t_{10} .³⁴ In the present case of a triplet ground state and quintuplet excited state the width is given by the relation $\delta\omega \approx \frac{3}{5} t_{10}^{-1} \propto e^{\Delta/kT}$ and using the measured values of t_{10} ⁸ and Δ ⁵ we estimate the width of each of the five excited levels to be $\sim 3\text{ cm}^{-1}$. As mentioned earlier this width increases at higher temperatures due to phonon-induced transitions.

The sum of the widths deduced from mechanisms (a)-(c) is $\sim 7\text{ cm}^{-1}$ which is in satisfactory agree-

ment with the measured value of 9 cm^{-1} .⁵ There is, of course, an uncertainty in the estimate of lifetime broadening [mechanism (c)] by a factor of about 3 due to uncertainties in extracting the Or-

bach contribution from the relaxation-time measurements. Further, as we have seen, the strain broadening [mechanism (b)] varies between samples by at least a factor of 3.

¹P. G. Klemens, in *Solid State Physics*, edited by H. Ehrenreich, F. Seitz, and D. Turnbull (Academic, New York, 1958), Vol. 7.

²Strictly one should distinguish between phonons which are energy eigenstates of the lattice, and traveling wave packets encountered in the theory of thermal conductivity, however, we shall follow the usual practice of using both terms indiscriminately. K. W. H. Stevens, Rept. Progr. Phys. **30**, 189 (1967).

³R. Berman and J. F. C. Brock, Proc. Roy. Soc. (London) **A289**, 46 (1966).

⁴M. F. Lewis and I. P. Morton, Phys. Letters **27A**, 547 (1968).

⁵J. Y. Wong, Phys. Rev. **168**, 337 (1968).

⁶G. A. Slack, Phys. Rev. **134**, A1268 (1964).

⁷G. A. Slack and S. Galgaitis, Phys. Rev. **133**, A253 (1964).

⁸J. B. Jones and M. F. Lewis, Solid State Commun. **5**, 595 (1967); **5**, 845 (1967); R. G. Leisure and D. I. Bolef, Phys. Rev. Letters **19**, 957 (1967); R. L. Hartmann, E. L. Wilkinson, and J. G. Castle, Jr., Phys. Rev. **171**, 299 (1968).

⁹A recent report observes similar effects in ZnS and CdTe and employs a similar analysis, but does not directly use measured spin-lattice relaxation times. G. A. Slack, General Electric Report No. 66C481 (unpublished).

¹⁰J. Callaway, Phys. Rev. **113**, 1046 (1959).

¹¹G. A. Slack, Phys. Rev. **126**, 427 (1962).

¹²T. H. K. Barron *et al.*, Proc. Roy. Soc. (London) **A250**, 70 (1959).

¹³R. Orbach, Phys. Rev. Letters **8**, 393 (1962).

¹⁴R. Orbach, thesis, University of California, 1960 (unpublished).

¹⁵W. Low, in *Solid State Physics*, edited by H. Ehrenreich, F. Seitz, and D. Turnbull (Academic, New York, 1960), Suppl. to Vol. 10.

¹⁶R. L. Scott and C. D. Jeffries, Phys. Rev. **127**, 32 (1962).

¹⁷F. S. Ham (private communication).

¹⁸A further assumption implicit in our arguments is that the strains at the Fe^{2+} sites in MgO are random over a distance equal to the thermal phonon mean free path in the undoped MgO. If this were not so, the effective spin line shape for intersection of a phonon would become the

spin-packet line shape rather than the inhomogeneously broadened envelope shape. The widths of these line-shape functions are probably a factor of 2 different for $\text{MgO}:\text{Fe}^{2+}$ (see Appendix). In our calculations, this assumption has produced good agreement with experiment, and we have found no evidence to support Shiren's conclusion that the strains at the Fe^{2+} sites are correlated over distances $\gtrsim 10^{-4}\text{ cm}$: N. S. Shiren, Phys. Rev. **128**, 2103 (1962). Indeed such discrepancies as remain between our calculations and experiment would become worse if we included such a correlation.

¹⁹D. G. Hughes and D. K. C. McDonald, Proc. Phys. Soc. (London) **78**, 75 (1961).

²⁰J. M. Ziman, *Electrons and Phonons* (Oxford U. P., Oxford, England, 1960).

²¹P. Carruthers, Rev. Mod. Phys. **33**, 92 (1961).

²²I. S. Ciccarello and K. Dransfeld, Phys. Rev. **134**, A1517 (1964).

²³M. F. Lewis, Cryogenics **10**, 38 (1970).

²⁴The experiments of L. J. Challis, M. A. McConachie, and D. J. Williams indicate the chromium impurities can give strong point-defect scattering effects which are dependent on the amount and valency of iron impurities and so E_P may well have a more complicated dependence upon N_s . L. J. Challis, M. A. McConachie, and D. J. Williams, Proc. Roy. Soc. (London) **A308**, 355 (1968).

²⁵C. Kittel, *Introduction to Solid State Physics* (Wiley, New York, 1966), p. 517.

²⁶R. Orbach, Phil. Mag. **5**, 1303 (1960).

²⁷R. T. Harley and H. M. Rosenberg, Proc. Roy. Soc. (London) **A315**, 551 (1970).

²⁸F. K. Lotgerin, J. Phys. Chem. Solids **23**, 1153 (1962).

²⁹R. J. Elliott and J. B. Parkinson, Proc. Phys. Soc. (London) **92**, 1024 (1967).

³⁰E. R. Feher, Phys. Rev. **136**, A145 (1964).

³¹D. H. McMahon, Phys. Rev. **134**, A128 (1964).

³²M. F. Lewis and A. M. Stoneham, Phys. Rev. **164**, 271 (1967).

³³F. S. Ham, Phys. Rev. **160**, 328 (1967).

³⁴R. Orbach, Proc. Roy. Soc. (London) **264**, 458 (1961). Our measured values of t_{10} are in good agreement with the calculated values of Ham (Ref. 33).